Check for updates

Water Practice & Technology

IWA PUBLISHING

© 2021 The Authors

Water Practice & Technology Vol 16 No 4, 1265 doi: 10.2166/wpt.2021.066

Photo-catalytic dye degradation of methylene blue by using ZrO_2/MWCNT nanocomposites

Akshatha Gangadhar [a,b,*], Abhilash Mavinakere Ramesh[a,b], Jagadish Krishnegowda[b,c] and Srikantaswamy Shivanna[a,b]

[a] Department of Studies in Environmental Science, University of Mysore, Manasagangotri, Mysore 570 006, India
[b] Centre for Materials Science and Technology, Vijinana Bhavan, University of Mysore, Manasagangotri, Mysore 570 006, India
[c] Department of Chemistry, Yuvaraja's College, University of Mysore, Manasagangotri, Mysore 570 005, India
*Corresponding author. E-mail: akshu.akshatha24@gmail.com

AG, 0000-0002-1706-5658

ABSTRACT

Photocatalytic degradation of the dyes was deliberated by altering the catalyst and dye concentrations. The Zirconium oxide/multiwall carbon nanotube (ZrO_2/MWCNT) catalyst was facilely synthesized by a hydrothermal synthesis method. The nanocomposite ZrO_2/MWCNT was formed in hydrothermal condition 95 °C of low growth temperature. The physico-chemical properties were successfully characterized using X-ray diffraction (XRD), scanning electron microscope (SEM), energy dispersive spectroscopy (EDS), dynamic light scattering (DLS) analysis, and X-ray photoelectron spectroscopy (XPS). The presence of Orbicular shaped ZrO_2 nanocrystallines and multiwall carbon nanotubes was characterized by XRD pattern, and shows the presence of ZrO_2 and MWCNT with the 2θ peaks at 19.62, 22.5 & 30.2. The thermal behavior of the ZrO_2/MWCNT partials was also investigated by differential thermal analysis, and their vibrational bands were identified by infrared spectroscopy. The photo catalytic degradation of methylene blue in industrial wastewater was observed under UV light irradiation using the synthesized ZrO_2/MWCNT as catalyst. The results revealed that the ZrO_2/MWCNT nanoparticles exhibited high degeneration with COD and TOC reducing from 241 mg/L and 148.00 mg/L to 2.34 mg/L and 1.26 mg/L respectively with an efficiency of 90–94% over 25–60 min duration of UV irradiation. In comparison with the pristine Zirconium oxide and MWCNT, the composite ZrO_2/MWCNT nanoparticles exhibited more efficient, durable and stable photo-catalytic activity during experiments.

Key words: methylene blue, multiwall carbon nanotube (MWCNT), photocatalytic activity, Zirconium oxide

HIGHLIGHTS

- The ZrO_2/MWCNT nanoparticles exhibited high degeneration efficiencies (90–94%) for 25–60 min of UV irradiation time.
- The ZrO_2/MWCNT nanocomposite exhibits a highly structural uniqueness combined with hydrothermal method and has an large surface area.
- The present investigation serves as a base-line data for future studies on ZrO_2/MWCNT nanocomposites for wastewater treatment.

This is an Open Access article distributed under the terms of the Creative Commons Attribution Licence (CC BY 4.0), which permits copying, adaptation and redistribution, provided the original work is properly cited (http://creativecommons.org/licenses/by/4.0/).

Downloaded from http://iwaponline.com/wpt/article-pdf/16/4/1265/944199/wpt0161265.pdf
by guest

GRAPHICAL ABSTRACT

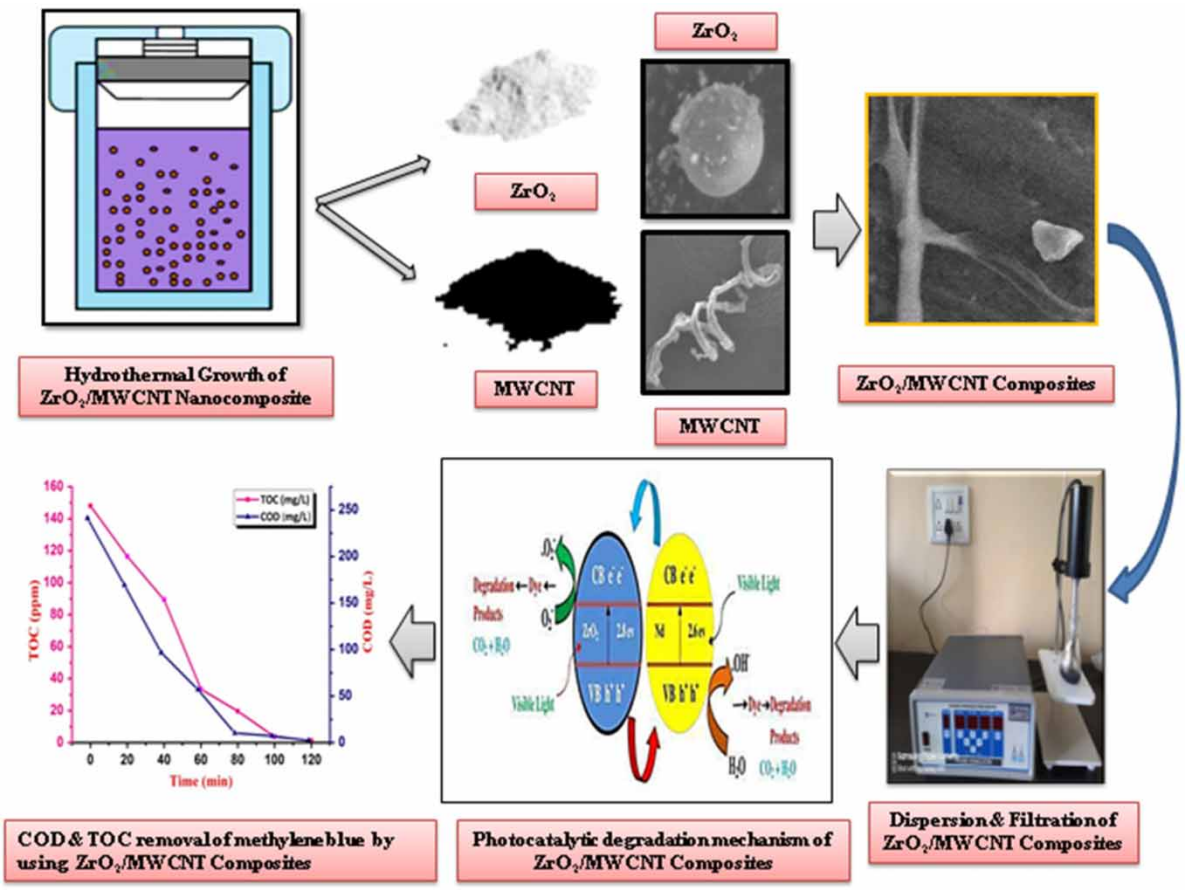

1. INTRODUCTION

According to the investigation by World Health Organization, about 1.8 billion people worldwide are still using contaminated water (Abhilash *et al.* 2019a). Hence, the strongest challenge to the international community has led mankind to energy-intensive water extraction and treatment processes (Abinaya *et al.* 2021). Among them, photocatalysis has drawn attention from the scientific community to contribute to the best solution for wastewater treatment-associated problems (Amin *et al.* 2014). Photocatalysis and its associated technologies offer excellent and environmentally-friendly removal of organochemical pollutants (Abhilash *et al.* 2019b). Photocatalysis is a method that involves breaking down or decomposition of varied dyes, organic dirt, and biological species such as harmful fungi and viruses on surfaces with using UV or light irradiation to make it clean (Butt 2020). Many procedures have been used for dye degradation including chemical oxidation, flocculation, chemical coagulation, membrane filtration, and biological degradation (Chanikya *et al.* 2021). These methods have their own disadvantages, and none is effective in completing the degradation of dyes used for coloring from wastewater (Bharath *et al.* 2020). Most of these techniques need sophisticated instrumentality and involve high prices, obstructing their application. Therefore, a cheap and environmentally friendly methodology is required to get rid of the contamination caused by wastewater (Ghazanfari *et al.* 2021). Among all the methods, nanoscience and nanotechnology are attractive and emerging areas of research. Nanoparticles own numerous improved properties such as smaller size, uniform size distribution, higher surface area, and high thermal and electrical conductivity (Wahab *et al.* 2018; Priya *et al.* 2020). Zirconium oxide nanoparticles (ZrO_2) have attracted significant interest as a highly active catalytic material for wastewater treatment (Liu *et al.* 2018), mainly because of their excellent properties, like biocompatibility, chemical inertness, outstanding chemical and thermal stability, good corrosion resistance, and a high isoelectric point, complete degradation of contaminants, and no secondary pollution (Naghipour *et al.* 2018; Ahmad *et al.* 2019; Yazdi *et al.* 2018). However they have high electrical conductivity. In particular, MWCNT is considered to be a highly suitable dopant because of its advantages, including

Downloaded from http://iwaponline.com/wpt/article-pdf/16/4/1265/944199/wpt0161265.pdf
by guest

high catalytic activity, good electrochemical properties, high-temperature resistance, and eco-friendly nature (Jagadish *et al.* 2018). Specifically, Zr^{4+} ions can replace carbon ions in the ZrO lattice, promoting strong interactions between Zr and C atoms and leading to Zr-C-O systems with enhanced electronic and catalytic activities (Ahmad *et al.* 2019; Sadiković & Nigović 2017). Numerous synthetic strategies, including hydrothermal routes, have been widely exploited for the controlled synthesis of ZrO_2/MWCNT with tunable sizes and morphologies (Yasin *et al.* 2016). Such a composite is more efficient, because of its simple process, high purity and homogeneity of samples, and low cost with high sensitivity (Sadiković 2017; Priya *et al.* 2020). nanocatalyst played important role in photoexcitation of electrons – hole pairs with high catalytic activity under visible light irradiation. The reason for such behavior is due to the fact that MB is a cation dye (Naghipour *et al.* 2018), and this can also be attributed to the fact that at higher pH value the surface charges of the adsorbent have become more negatively charged (Balarak *et al.* 2015; Jaafari *et al.* 2020; Ramesh *et al.* 2020). The formation of a highly stable, readily storable, compact ZrO_2/MWCNT, composite may provide a new pathway for the purification of effluent (Sharma *et al.* 2018; Serpone 2000; Ramesh & Shivanna 2021). It should be pointed out that from our simulations, the adsorption of dye occurs with ZrO_2/MWCNT, which forms hydrogen bonds and weak van der Waals interactions (Verlicchi & Ghirardini 2019). The XRD and SEM characterization provides fundamental evidence of the high yield and purity of composite preparation (Dagar & Narula 2017; Assis *et al.* 2019). UV-visible spectroscopy, the EDS test, and DLS are accurate, convenient, and rapid characterization tools for monitoring the adsorption and pollution removal process in aqueous systems (Kassem *et al.* 2019; Higashiwaki & Fujita 2020; Kharlamova & Eder 2020).

In this work the attempt is made to synthesize ZrO_2/MWCNT nanocomposite by a hydrothermal method. The study aims to determine the photocatalytic degradation of methylene blue using synthesized rare orbicular shaped ZrO_2/MWCNT nanocomposite as catalyst. It is observed that the synthesized composite works effectively to reduce the COD and TOC concentration to a great extent. This exceptional combination of nanocatalyst was found to be more efficient, durable and stable when compared to the pristine ZrO_2 and less study has been made in this direction.

2. MATERIAL AND METHODOLOGY

2.1. Zirconyl chloride octahydrate ($ZrOCl_2$*$8H_2O$)

Zirconyl chloride is an inorganic compound with the formula of $[Zr_4(OH)_8(H_2O)_{16}]Cl_8(H_2O)$, more commonly written $ZrOCl_2$ *$8H_2O$, and referred to as zirconyl chloride octahydrate. It is a white solid and is the commonest soluble by-product of atomic number 40. The $ZrOCl_2$*$8H_2O$ was purchased from (Sigma Aldrich, India) (Sadiković 2017). Polystyrene is a polymeric compound, potassium hydroxide AR (CDH, fine chemical, India), dichloromethane, sodium hydroxide (NaOH), ferric chloride (97%, Fe 21.6%, Sigma Aldrich, India), and nitric acid (Sigma Aldrich, India).

2.2. Synthesis of Zirconium oxide

Take a 50 ml conical flask with 20 ml of distilled water. Add 0.1 M of zirconyl chloride octahydrate ($ZrOCl_2$ *$8H_2O$) and dissolve it with effective stirring. After few minutes, add 0.2 M of potassium hydroxide (KOH) dissolved in 5 ml of distilled water. After some time precipitation occurs, then the solution was transferred into a stainless-steel Teflon lined sterilized container of 15 ml and kept in an oven at 180 °C for 16 h (Kronka *et al.* 2021). To remove the soluble impurities and depress agglomeration, the ensuing precipitates square measure was cleansed with water and absolute alcohol. The final product was dried for 3 h in a vacuum at 80 °C.

2.3. Synthesis of multiwall carbon nanotubes

Polystyrene was used as the carbon source for the growth of MWCNT, dichloromethane was used as a solvent to dissolution of polystyrene to influence the synthesis of MWCNT. Sodium hydroxide was used as a chemical activation agent to activate hydrocarbon. Ferric chloride was used as a catalyst under hydrothermal reaction. In a typical synthesis, 1.5 g of powdered polystyrene was added to 30 ml dichloromethane. The solution mixture was kept in a magnetic stirrer for 30 min at laboratory temperature, then 8 ml of the above solution mixture was transferred into 20 ml capacity Teflon liner, further 6 ml of 20% sodium hydroxide solution was added to the mixture and 0.25 g of dried ferric chloride was added. The Teflon liner was closed and placed in the stainless steel autoclave was placed in hot air oven which was fixed tightly. Further the autoclave was placed in hot air oven and heated (120–160 °C) for different temperature and different duration (10–24 hr) (Jagadish *et al.* 2016).

Downloaded from http://iwaponline.com/wpt/article-pdf/16/4/1265/944199/wpt0161265.pdf
by guest

2.4. Zirconium oxide/MWCNT composite synthesis method

Synthesized multiwall carbon nanotubes were purified by refluxing the as-received sample in 10 wt.% nitric acid for 12 h. The acid-treated, dispersed MWCNT was then collected by filtration and dried at 120 °C for 12 h in vacuum. A typical synthesis process of the ZrO_2/MWCNT nanocomposite is described as follows. Firstly, 0.1 g MWCNT was dispersed in 25 ml deionized [DI] water by ultrasonic vibration for 2 h. Then, 0.3 g ZrO_2 was added into the above suspension, and the mixed solution was stirred by a magnetic bar for 2 h. After that, the mixed solution was transferred to a 30-mL, Teflon-lined, stainless steel autoclave. The autoclave was sealed and put in an electric oven at 150 °C for 6 h and then naturally cooled to room temperature. After the hydrothermal treatment, the resultant samples were collected by filtration and washed with DI water. ZrO_2/MWCNT nanocomposites were finally dried in an oven at 100 °C for 12 h for further characterization.

2.5. Photocatalytic degradation mechanism of dye using doped ZrO_2/MWCNT

The designed ZrO_2/MWCNT is evaluated by degradation of methylene blue dye (250 ml of textile effluent). The different initial concentration of ZrO_2/MWCNT was considered for performing the degradation experiment as shown in Figure 1 with 5 mg of ZrO_2/MWCNT nanoparticles. The experiment was carried out in a UV light radiation cabinet (model No.EQ780). A150 W Xenon lamps were used as light sources; the standard distance was maintained between the UV source and reaction vessel, which is about 5–15 cm. Before starting the reaction, the suspension was stirred using a magnetic stirrer in the darkroom for 30 min, then the reaction setup was exposed to a UV cabinet under normal conditions (Lombardo *et al.* 2016; Abhilash *et al.* 2019b). The sample was taken to calculate the photodegradation efficiency of methylene blue using:

$$\text{Removal efficacy} = \frac{C_o - C}{C_o} \times 100$$

where C_o is the initial concentration of methylene blue and C is the concentration of dye after degradation.

It was necessary to measure the chemical oxygen demand (COD) and total organic carbon (TOC) to assess the purity of the degraded dyes before discharging. Total organic carbon (TOC) analysis was performed to understand and estimate the extent of mineralization of MB throughout the strategy. The photocatalytic degradation methodology may result in the disappearance of color. This study discloses that the color disappearance of the dye was quicker than the degree of mineralization with most TOC removal. This processed that the dye molecules were reinvigorated to totally different intermediates and that the dye was systematically decolorized in up to

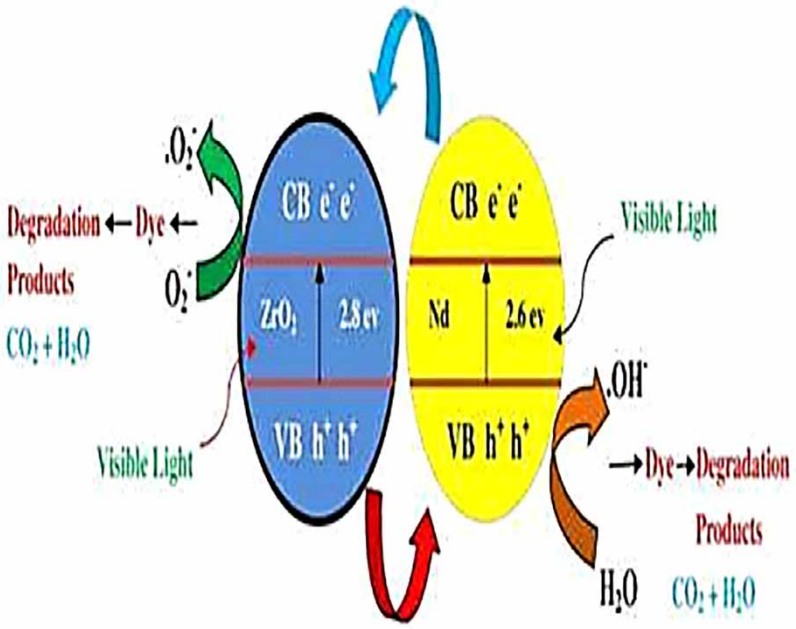

Figure 1 | Photocatalytic degradation mechanism of methylene blue dye.

Downloaded from http://iwaponline.com/wpt/article-pdf/16/4/1265/944199/wpt0161265.pdf
by guest

120 min, which could cause complete mineralization. Similarly, the reduction of COD reflects the extent of removal or mineralization of associate organic species; the proportion of change in COD and TOC throughout photo-removal was measured as beneath optimum reaction conditions [concentration 9 metric long measure, catalyst concentration 0.75 g, pH scale 5 and irradiation time of up to 120 min]. The solutions obtained after 120 min of photo-removal showed an enormous decrease in COD and TOC concentration.

3. RESULTS AND DISCUSSION

3.1. Scanning electron microscope (SEM)

Figure 2 shows the characteristic SEM images of ZrO_2 and MWCNTs and ZrO_2 /MWCNT composites. The untreated MWCNTs were observed and has an their outer diameter in the range of <10 nm with tubular structures, Zirconium oxide has an orbicular shaped nanostructure. Prior to the modification of the composite, it was possible to identify in the micrographs during ultrasonication that the MWCNTs were combined with the ZrO_2. These SEM images were taken for the material at pH 4 (acidic condition) in which adsorption was greater. The adsorbent (ZrO_2/MWCNT) morphologies (Almaev *et al.* 2021).

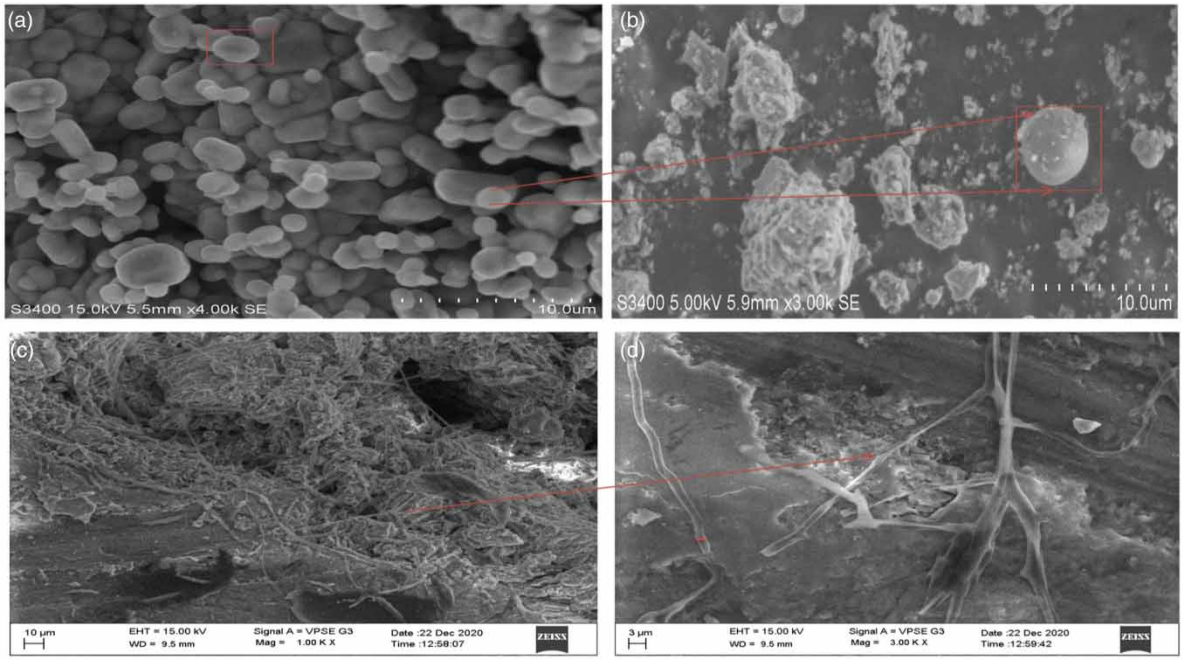

Figure 2 | Scanning electron microscope (SEM) images of the grown (a) and (b) ZrO_2 and (c) MWCNT and (d) ZrO_2/MWCNT nanostructures via hydrothermal method with different growth temperatures.

3.2. X-ray photoelectron spectroscopy (XPS) analysis

The chemical composition of the prepared ZrO_2/MWCNT composites and chemical prominence of elements was confirmed by XPS analysis to compare the purity of the surface and the degree of oxidation, to gain vision of the shape evolution and to unravel the formation mechanism of the samples. The spectrum shows (Figure 3) that the ZrO_2/MWCNT composite consists of Zr, O and C elements. The corresponding high-resolution XPS spectra are provided in Figure 3. The results show the presence of a large amount of carbon. The C 1s spectrum shows three deconvoluted peaks at 282.92, 284.68 and 286.10 eV that could be endorsed to the sp2 C – C, C – O and N – C – N bond in the composite, respectively. The peaks of Zr and O are clearly visible, indicating that the samples were greatly pure. The core-level binding energies of Zr 3d, and O 1, which have been corrected for the surface charging effect, were determined from the respective XPS spectra. High-resolution Zr 3d, and O 1s, XPS spectra were taken of the synthesised samples. An analysis of the XPS results shows a strong effect on both the Zr and O atoms. The Zr 3d peak is identified at 182 and 188 eV in the spectra of the samples respectively, which suggests the presence of material that is metallic in nature. These results of electron

Downloaded from http://iwaponline.com/wpt/article-pdf/16/4/1265/944199/wpt0161265.pdf
by guest

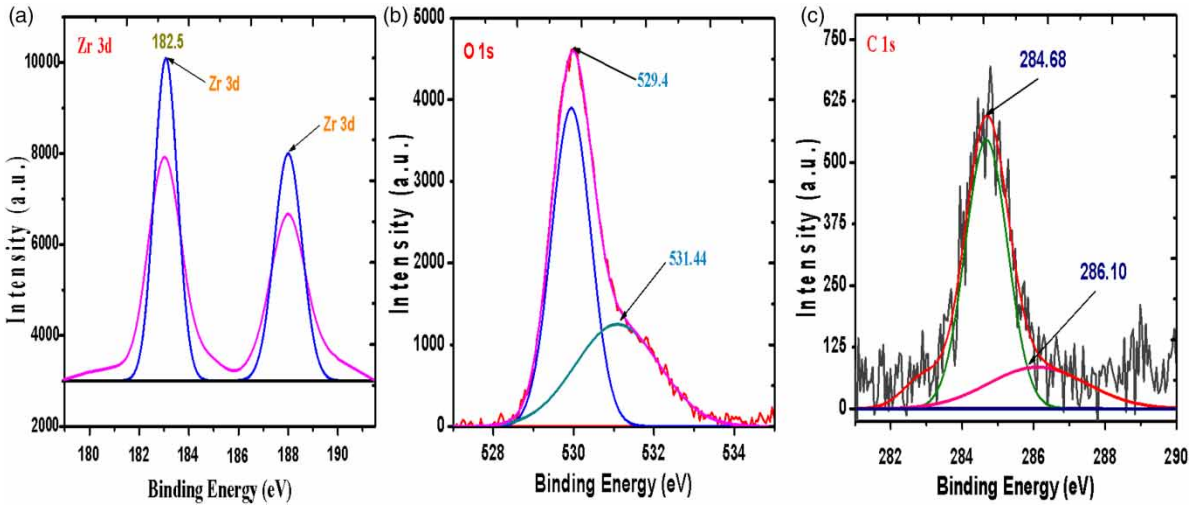

Figure 3 | XPS pattern of (a) binding energy of Zr 3d; (b) binding energy of O 1s; (c) binding energy of C1s.

irradiation show that structural grey metal has a tendency to absorb electrons. The high-resolution O 1s spectra could be fitted into three peaks at 530.6, 531.7 and 532.8 eV. The peak at 530.6 eV could be attributed to the oxygen in OH group or water species adsorbed by the composite. The peaks with the binding energy of 531.7 and 532.8 eV could be assigned to the oxygen in ZrO_2 and O – C, respectively.

3.3. Dynamic light scattering (DLS)

DLS is the most helpful technique for characterizing nanomaterials in solutions, attributable to the Brownian movement of particles. The particle sizes of dispersed MWCNT were analyzed by using DLS. The untreated ZrO_2/MWCNT has an average particle size of 23–87 nm, as shown in Figure 4. Zeta potential was calculated using DLS, which explains the stability of MWCNT in solutions by having an absolute value greater than 30 nmV.

3.4. Energy dispersive X-ray spectroscopy (EDS)

Energy dispersive spectroscopy (EDS) analysis confirmed the phase purity of the MWCNT/ZrO_2 photo-catalyst, as shown in Figure 5. Based on theoretical calculations, a certain amount of Zirconyl chloride octahydrate was

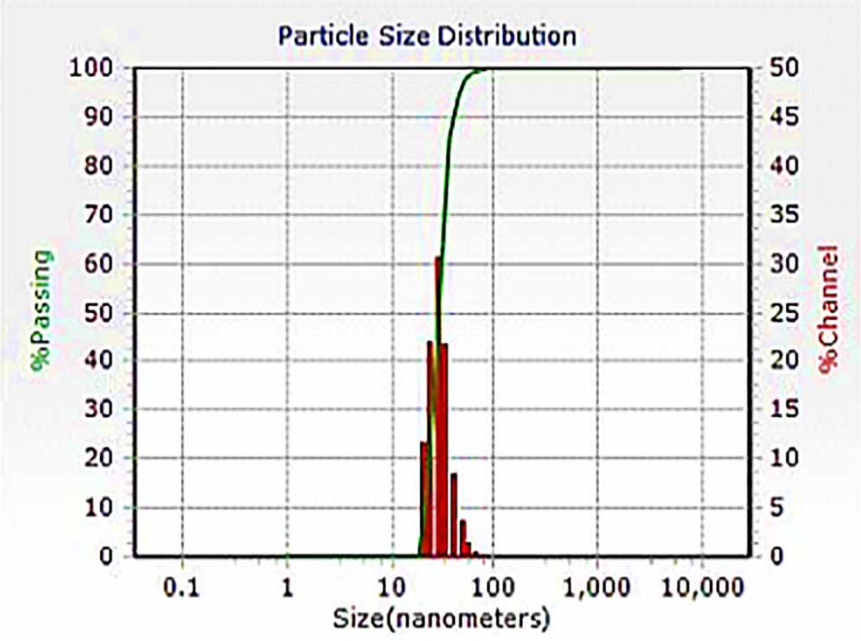

Figure 4 | Dynamic Light Scattering (DLS) images of the grown MWCNT/ ZrO_2 nanostructures via hydrothermal method with different growth temperatures.

Downloaded from http://iwaponline.com/wpt/article-pdf/16/4/1265/944199/wpt0161265.pdf
by guest

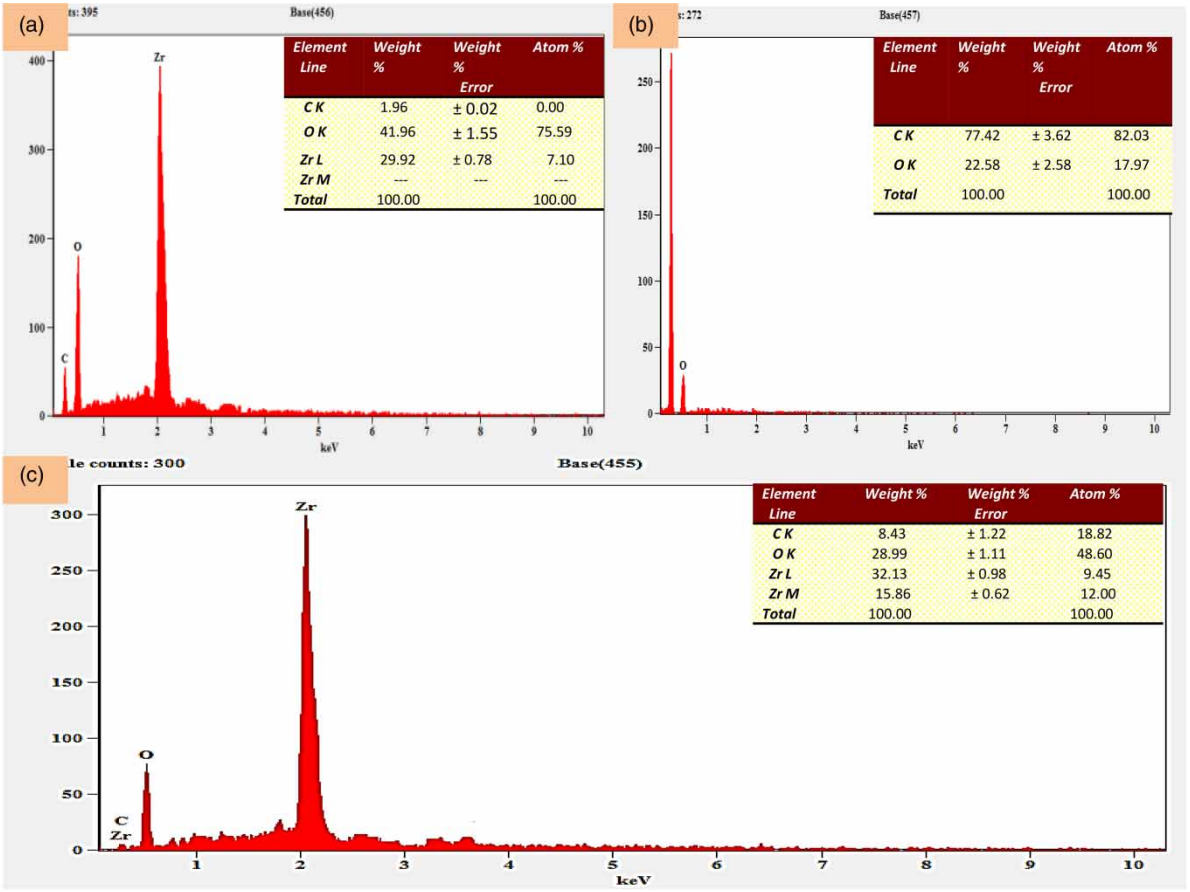

Figure 5 | Energy Dispersive X-Ray spectroscopy (EDS) images of (a) ZrO_2, (b) MWCNT and (c) ZrO_2/MWCNT nanostructures via hydrothermal method.

used in the synthesis of the nanocomposite. However, EDS analysis revealed that the amount of ZrO_2 formed in the final product was 29.92 wt(%) for the optimized sample. The excess amount of unrelated ZrO_2 salt was filtered out during the washing process. The elemental composition of the ZrO_2/MWCNT photo-catalyst, the average particle size distribution measurement of the ZrO_2/MWCNT photo-catalyst are shown in (Figure 5) The particle sizes are distributed in the range of fill scale count 395 nm, and the average particle size is about 69.55 wt (%). The stability analysis of the ZrO_2/MWCNT particles in de-ionized water suspension was carried out by zeta potential measurement.

3.5. X-ray diffraction (XRD) of ZrO_2/MWCNT composites

The crystalline study of ZrO_2/MWCNT composites was investigated by powder XRD (Figure 6). The XRD pattern revealed the peaks related to MWCNT and ZrO_2. In the XRD pattern, among the peaks the strongest direction angles at $2\theta = 19.62^0$ can be indexed to the (111) reaction of the circular structure. The sharpness of the peak at the angle $2\theta = 22.5^0$ indicates the graphite structure of the MWCNT without significant damage in the composite material. The other characteristic diffraction peak at $2\theta = 20.1^0$ and 30.2^0 is associated with the C (100) diffraction of MWCNT (which corresponds to a crystalline orthorhombic lattice), which indicates the semi-crystalline nature of the ZrO_2 present in the composite material.

3.6. UV-Vis spectroscopy

The dispersed and individual MWCNT are active in the UV-Vis region by exhibiting characteristic bands between 200 and 1,200 nm. It is possible to characterize dispersed MWCNT and ZrO_2 by UV-Vis spectroscopy. Figure 7 depicts the UV-Vis spectra of dispersed MWCNT and ZrO_2 obtained through hydrothermal reactions in supercritical conditions of respective organic solvents and standard (untreated) MWCNT. The absorbance of MWCNT was recorded for the prepared solution.

Downloaded from http://iwaponline.com/wpt/article-pdf/16/4/1265/944199/wpt0161265.pdf
by guest

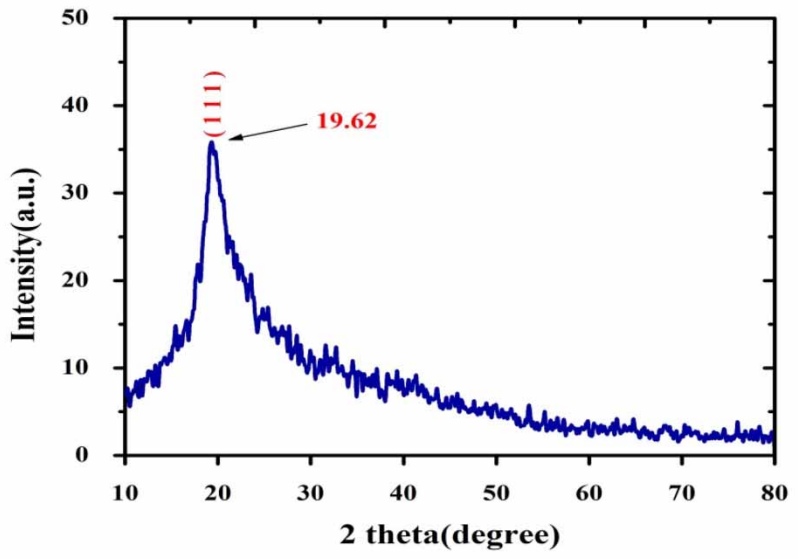

Figure 6 | X-ray diffraction (XRD) of samples calcinated at different temperatures. 2θ scanned X-ray diffraction (XRD) patterns of the as-prepared a) ZrO_2 /MWCNT nanocomposite.

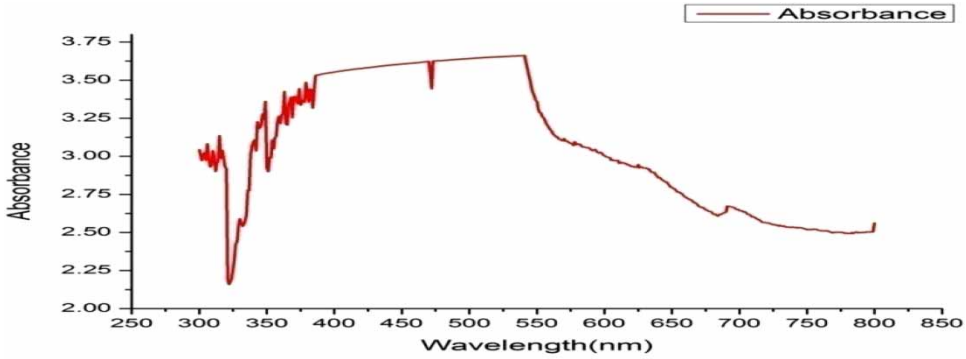

Figure 7 | UV-Vis spectroscopy images of the grown ZrO_2/MWCNT nanostructures via hydrothermal method with different growth temperatures.

3.7. Photo-catalytic degradation of industrial wastewater using ZrO_2/MWCNT

Photocatalytic of methylene blue dye degradation by various heterogeneous semiconductor materials such as Zirconium oxide, doped with MWCNT, is considered as an irreversible process since there exists no equilibrium between the dye solution and the photocatalyst. Initially, no dye degradation occurs at a time interval ($t = 0$). But with increase in regular time interval, dye degradation occurs; in the presence of a visible light source radiation the adsorption of dye occurs with ZrO_2/MWCNT, in which electron transfer will take place, form hydrogen bonds will form and weak vander Waals interactions will occur. Consequently, the degradation occurred to allow dye molecules to move from solitary explication to the material interface and subsequently to carbon dioxide (CO_2), and water (H_2O). Maximum degradation occurs at the equilibrium time ($t = 120$ min) by the photocatalyst. The photodegradation process of COD removal is 90–94% (Figure 8) and TOC removal is 87–96% of degradation using heterogeneous photocatalysts as considered by Langmuir–Hinshelwood first-order kinetics model. The nonlinear form of Langmuir–Hinshelwood first order kinetic model is expressed as follows.

In general, the photocatalytic activity of a metal oxide semiconductor depends on a number of factors, such as particle size, morphologies and surface properties. Pure ZrO_2 was subjected to photocatalytic activity with methylene blue dye. The band-gap of pure ZrO_2 is 2.8 eV and that of MWCNT doped ZrO_2 is 2.6 eV. The lower band-gap of 2.6 eV in MWCNT-doped ZrO_2 shows more ability to absorb UV light when compared to

Downloaded from http://iwaponline.com/wpt/article-pdf/16/4/1265/944199/wpt0161265.pdf
by guest

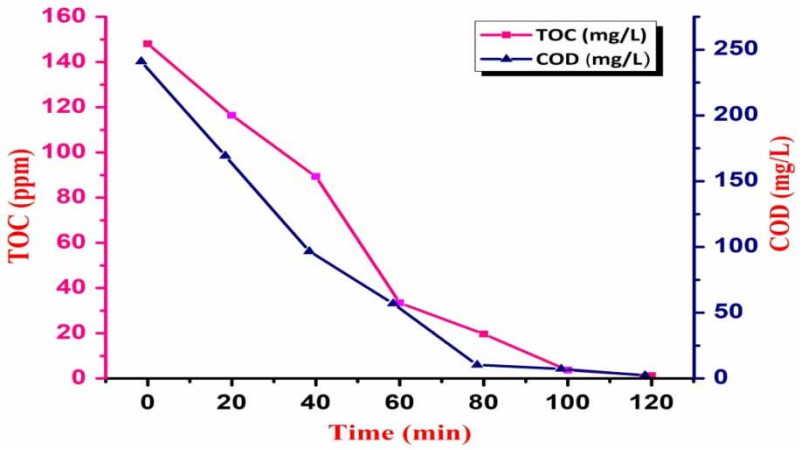

Figure 8 | Photo-degradation of methylene blue using ZrO_2/MWCNT photo-catalysts.

pure ZrO_2 with a band gap of 2.8 eV. Though the band-gap decreased on adding ternary and quaternary elements, the photocatalytic activity was not effective due to the formation of three or more metal oxide nanocomposites. Though mixed metal oxide nanocomposites are formed, they contribute to some extent to the photodegradation of MB dye.

3.8. Adsorption kinetic study

For the adsorption process, it is a very essential parameter to determine the rate of time at which the adsorbate is removed from aqueous solution using the unit mass of adsorbent. The adsorbate concentration in aqueous solution can be measured at a certain time, qt (mgg^{-1}), which was determined by Equation (1):

$$q_t = \frac{C_o - C_t}{M} \times V \tag{1}$$

where C_t (mgL^{-1}) is a concentration of adsorbate in aqueous solution at a certain time t (h).

The following equations were used for fitting the adsorption kinetics.

For the pseudo-first-order kinetic model,

$$\log(q_e - q_t) = \log q_e - \frac{K_1}{2.303} t \tag{2}$$

For the pseudo-second-order kinetic model:

$$\frac{t}{q_t} = \frac{1}{K_2 q_e^2} + \frac{t}{q_e} \tag{3}$$

where K_1 (min^{-1}) is the rate constant of the pseudo-first-order and K_2 ($g^{-1}\,mg^{-1}\,min^{-1}$) is the rate constant of pseudo-second-order adsorption kinetics, respectively. q_e (mgg^{-1}) and q_t (mgg^{-1}) are the amounts of adsorbate adsorbed at equilibrium and time 't', respectively. K_{int} ($mg^{-1}\,min^{-1/2}$) denotes the intraparticle diffusion rate constant and C (mg^{-1}) was the thickness of the boundary layer of adsorbate onto adsorbent sites.

The rate constants obtained are linear within the plot of 'log ($q_e - q_t$) vs. time' and this linearity, which resembles pseudo-first-order reaction kinetics, was obtained from Equation (2). If a linear relationship is found, then k_1 and projected q_e is determined from the slope and intercept of the plot (Figure 9), correspondingly. For the surface assimilation of MB, it has been detected that the pseudo-first-order equation fits well for the primary 90 min of contact time of dye with the adsorbent and then the data deviates from the theory. Thus, it is evident that the initial stages were based on rapid adsorption and follow pseudo-first order reaction kinetics (Table 1).

Downloaded from http://iwaponline.com/wpt/article-pdf/16/4/1265/944199/wpt0161265.pdf
by guest

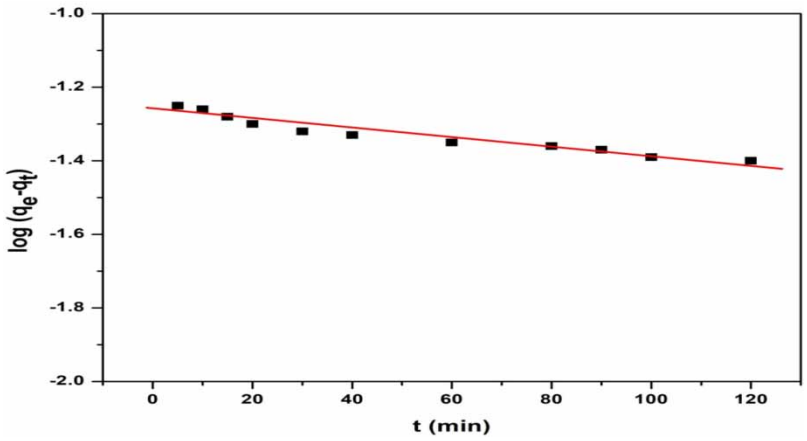

Figure 9 | Adsorption kinetic of ZrO_2/MWCNT for the adsorption of methylene blue dye.

Table 1 | Adsorption kinetic of dye onto ZrO_2/MWCNT adsorbent

			Pseudo-first-order			Pseudo-second-order		
Adsorbents	**C_0 (mg/L)**	**q_e,exp (mg/g)**	**K_1 (min^{-1})**	**q_e,cal (mg/g)**	**R^2**	**K_2 (g/mg min^{-1})**	**q_e, cal (mgg^{-1})**	**R^2**
ZrO_2/MWCNT	10	1.22	1.15	0.88	0.98	0.006	0.158	0.99

4. CONCLUSION

ZrO_2/MWCNT nanocomposite was successfully synthesized by a simple hydrothermal process for efficient organic pollutant dye removal. The structural, morphological, optical and thermal properties of the synthesized nanocomposite were extensively investigated using XRD, SEM, EDX, XPS, UV-Vis spectroscopy and DLS respectively. The XRD and XPS characterization provide fundamental evidence of the high yield and purity of composite preparation. The dye degradation results indicate that the synthesized ZrO_2/MWCNT works effectively in degrading the methylene blue dye at the optimum pH of 5, over a duration of 120 min. The COD and TOC values are 90–94% and 87–96% respectively. It is a rare approach to methylene blue dye degradation by using an orbicular-shaped nanomaterial. It is observed that this removal process is more efficient and is environmentally friendly, reusable, durable and also cost effective.

ACKNOWLEDGEMENT

Akshatha. G University of Mysore, acknowledges financial assistance through – Special Cell: (SC4/4/2020-21 dated: 18.03.2021).

DATA AVAILABILITY STATEMENT

All relevant data are included in the paper or its Supplementary Information.

REFERENCES

Abhilash, M. R., Akshatha, G. & Srikantaswamy, S. 2019a Photocatalytic dye degradation and biological activities of the Fe_2O_3/Cu_2O nanocomposite. *RSC Advances* **9**(15), 8557–8568.

Abhilash, M. R., Gangadhar, A., Krishnegowda, J., Chikkamadaiah, M. & Srikantaswamy, S. 2019 Hydrothermal synthesis, characterization and enhanced photocatalytic activity and toxicity studies of a rhombohedral Fe_2O_3 nanomaterial. *RSC Advances* **9**(43), 25158–25169.

Abinaya, S., Kavitha, H. P., Prakash, M. & Muthukrishnaraj, A. 2021 Green synthesis of magnesium oxide nanoparticles and its applications: a review. *Sustainable Chemistry and Pharmacy* **19**, 100368.

Ahmad, I., Islam, M., Parvez, S., AlHabis, N., Umar, A., Munir, K. S., Wang, N. & Zhu, Y. 2019 Reinforcing capability of multiwall carbon nanotubes in alumina ceramic hybrid nanocomposites containing zirconium oxide nanoparticles. *International Journal of Refractory Metals and Hard Materials* **84**, 105018.

Downloaded from http://iwaponline.com/wpt/article-pdf/16/4/1265/944199/wpt0161265.pdf
by guest

Almaev, A. V., Chernikov, E. V., Novikov, V. V., Kushnarev, B. O., Yakovlev, N. N., Chuprakova, E. V., Oleinik, V. L., Lozinskaya, A. D. & Gogova, D. S. 2021 Impact of Cr_2O_3 additives on the gas-sensitive properties of β-Ga_2O_3 thin films to oxygen, hydrogen, carbon monoxide, and toluene vapors. *Journal of Vacuum Science & Technology A: Vacuum, Surfaces, and Films* **39**(2), 023405.

Amin, M., Alazba, A. & Manzoor, U. 2014 A review of removal of pollutants from water/wastewater using different types of nanomaterials. *Advances in Materials Science and Engineering* **2014**, 1–24.

Assis, M. d., Robeldo, T., Foggi, C. C., Kubo, A. M., Mínguez-Vega, G., Condoncillo, E., Beltran-Mir, H., Torres-Mendieta, R., Andrés, J. & Oliva, M. 2019 Ag nanoparticles/α-Ag_2WO_4 composite formed by electron beam and femtosecond irradiation as potent antifungal and antitumor agents. *Scientific Reports* **9**(1), 1–15.

Balarak, D., Jaafari, J., Hassani, G., Mahdavi, Y., Tyagi, I., Agarwal, S. & Gupta, V. K. 2015 The use of low-cost adsorbent (Canola residues) for the adsorption of methylene blue from aqueous solution: isotherm, kinetic and thermodynamic studies. *Colloids and Interface Science Communications* **7**, 16–19.

Bharath, M., Krishna, B. & Manoj Kumar, B. 2020 Degradation and biodegradability improvement of the landfill leachate using electrocoagulation with iron and aluminum electrodes: a comparative study. *Water Practice & Technology* **15**(2), 540–549.

Butt, B. Z. 2020 Nanotechnology and waste water treatment. In: *Nanoagronomy* (B. Z. Butt & I. Naseer, eds). Springer, Cham, pp. 153–177.

Chanikya, P., Nidheesh, P., Babu, D. S., Gopinath, A. & Kumar, M. S. 2021 Treatment of dyeing wastewater by combined sulfate radical based electrochemical advanced oxidation and electrocoagulation processes. *Separation and Purification Technology* **254**, 117570.

Dagar, A. & Narula, A. K. 2017 Effect of nitrogen-doping on photo-catalytic activity of polypyrrole/zinc oxide/flyash cenosphere (PPY/ZnO/FAC) composite under visible light. *Journal of Materials Science: Materials in Electronics* **28**(12), 8643–8654.

Ghazanfari, S. Z., Jaafari, J., Ashrafi, S. D. & Taghavi, K. 2021 Decolourisation of direct red dye 81 from aqueous solutions by SnO_2/H_2O_2 hybrid process. *International Journal of Environmental Analytical Chemistry* **5**, 1–15.

Higashiwaki, M. & Fujita, S. 2020 *Gallium Oxide: Materials Properties, Crystal Growth, and Devices*, Vol. 293. Springer Nature, Tokyo, Japan.

Jaafari, J., Barzanouni, H., Mazloomi, S., Farahani, N. A. A., Sharafi, K., Soleimani, P. & Haghighat, G. A. 2020 Effective adsorptive removal of reactive dyes by magnetic chitosan nanoparticles: kinetic, isothermal studies and response surface methodology. *International Journal of Biological Macromolecules* **164**, 344–355.

Jagadish, K., Chandrashekar, B., Byrappa, K., Rangappa, K. & Srikantaswamy, S. 2016 Simultaneous removal of dye and heavy metals in a single step reaction using PVA/MWCNT composites. *Analytical Methods* **8**(11), 2408–2412.

Jagadish, K., Shiralgi, Y., Chandrashekar, B. N., Dhananjaya, B. L. & Srikantaswamy, S. 2018 *Ecofriendly Synthesis of Metal/Metal Oxide Nanoparticles and Their Application in Food Packaging and Food Preservation, in Impact of Nanoscience in the Food Industry*. Elsevier, Mysuru, Karnataka, p. 197–216.

Kassem, A., Ayoub, G. M. & Malaeb, L. 2019 Antibacterial activity of chitosan nano-composites and carbon nanotubes: a review. *Science of the Total Environment* **668**, 566–576.

Kharlamova, M. V. & Eder, D. 2020 Carbon nanotubes: synthesis, properties, and new developments in research. *Synthesis and Applications of Nanocarbons* **2**, 107–147.

Kronka, M. S., Cordeiro-Junior, P. J., Mira, L., dos Santos, A. J., Fortunato, G. V. & Lanza, M. R. 2021 Sustainable microwave-assisted hydrothermal synthesis of carbon-supported ZrO_2 nanoparticles for H_2O_2 electrogeneration. *Materials Chemistry and Physics* **124575**, 64–74.

Liu, D., Deng, S., Maimaiti, A., Wang, B., Huang, J., Wang, Y. & Yu, G. 2018 As(III) and As(V) adsorption on nanocomposite of hydrated zirconium oxide coated carbon nanotubes. *Journal of Colloid and Interface Science* **511**, 277–284.

Lombardo, P. C., Poli, A. L., Castro, L. F., Perussi, J. R. & Schmitt, C. C. 2016 Photochemical deposition of silver nanoparticles on clays and exploring their antibacterial activity. *ACS Applied Materials & Interfaces* **8**(33), 21640–21647.

Naghipour, D., Hoseinzadeh, L., Taghavi, K. & Jaafari, J. 2018 Characterization, kinetic, thermodynamic and isotherm data for diclofenac removal from aqueous solution by activated carbon derived from pine tree. *Data in Brief* **18**, 1082–1087.

Priya, R., Stanly, S., Dhanalekshmi, S. B., Mohammad, F., Al-Lohedan, H. A., Oh, W. C. & Sagadevan, S. 2020 Highly effective photocatalytic degradation of methylene blue using PrO_2–MgO nanocomposites under UV light. *Optik* **206**, 164318.

Ramesh, A. M. & Shivanna, S. 2021 Hydrothermal synthesis of MoO_3/ZnO heterostructure with highly enhanced photocatalysis and their environmental interest. *Journal of Environmental Chemical Engineering* **9**(2), 105040.

Ramesh, A. M., Gangadhar, A., Chikkamadaiah, M., Krishnegowda, J. & Shivanna, S. 2020 Synthesis of graphene nanosheets by emitted black carbon and its sustainable applications. *Journal of Environmental Chemical Engineering* **8**(5), 104071.

Sadiković, M. 2017 Development of electrochemical platform based on carbon nanotubes decorated with zirconium oxide nanoparticles for determination of nebivolol. *International Journal of Electrochemical Science*, 9675–9688.

Sadiković, M. & Nigović, B. 2017 Development of electrochemical platform based on carbon nanotubes decorated with zirconium oxide nanoparticles for determination of nebivolol. *International Journal of Electrochemical Science* **12**, 9675–9688.

Serpone, N. 2000 *Photocatalysis*. Kirk-Othmer Encyclopedia of Chemical Technology. Wiley & Sons, New York, NY.

Sharma, G., Soni, R. & Jasuja, N. D. 2018 Phytoassisted synthesis of magnesium oxide nanoparticles with *Swertia chirayaita*. *Journal of Taibah University for Science* **11**(3), 471–477.

Downloaded from http://iwaponline.com/wpt/article-pdf/16/4/1265/944199/wpt0161265.pdf
by guest

Verlicchi, P. & Ghirardini, A. 2019 Occurrence of micropollutants in wastewater and evaluation of their removal efficiency in treatment trains: the influence of the adopted sampling mode. *Water* **11**(6), 1152.

Wahab, R., Ahmad, N., Alam, M. & Ansari, A. A. 2018 Nanocubic magnesium oxide: towards hydrazine sensing. *Vacuum* **155**, 682–688.

Yasin, A. S., Mohamed, H. O., Mohamed, I. M. A., Mousa, H. M. & Barakat, N. A. M. 2016 Enhanced desalination performance of capacitive deionization using zirconium oxide nanoparticles-doped graphene oxide as a novel and effective electrode. *Separation and Purification Technology* **171**, 34–43.

Yazdi, M. N., Yamini, Y. & Asiabi, H. 2018 Multiwall carbon nanotube- zirconium oxide nanocomposite hollow fiber solid phase microextraction for determination of polyaromatic hydrocarbons in water, coffee and tea samples. *Journal of Chromatography A* **1554**, 8–15.

First received 5 May 2021; accepted in revised form 24 June 2021. Available online 7 July 2021

Downloaded from http://iwaponline.com/wpt/article-pdf/16/4/1265/944199/wpt0161265.pdf
by guest